


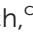




RESEARCH ARTICLE

[View Article Online](#)
[View Journal](#) | [View Issue](#)Cite this: *RSC Med. Chem.*, 2024, 15, 1773

Evaluation of ketoclofazone and its analogues as inhibitors of 1-deoxy-D-xylulose 5-phosphate synthases and other thiamine diphosphate (ThDP)-dependent enzymes†

Alex H. Y. Chan, ^{‡a} Terence C. S. Ho, ^{‡a} Imam Fathoni,^b Rawia Hamid, ^{cd}
Anna K. H. Hirsch, ^{cd} Kevin J. Saliba ^b and Finian J. Leeper ^{*a}

Most pathogenic bacteria, apicomplexan parasites and plants rely on the methylerythritol phosphate (MEP) pathway to obtain precursors of isoprenoids. 1-Deoxy-D-xylulose 5-phosphate synthase (DXPS), a thiamine diphosphate (ThDP)-dependent enzyme, catalyses the first and rate-limiting step of the MEP pathway. Due to its absence in humans, DXPS is considered as an attractive target for the development of anti-infectious agents and herbicides. Ketoclofazone is one of the earliest reported inhibitors of DXPS and antibacterial and herbicidal activities have been documented. This study investigated the activity of ketoclofazone on DXPS from various species, as well as the broader ThDP-dependent enzyme family. To gain further insights into the inhibition, we have prepared analogues of ketoclofazone and evaluated their activity in biochemical and computational studies. Our findings support the potential of ketoclofazone as a selective antibacterial agent.

Received 31st January 2024,
Accepted 27th March 2024

DOI: 10.1039/d4md00083h

rsc.li/medchem

Introduction

Isoprenoids, comprising a vast family of natural products, are key metabolic components of all organisms.¹ They are derived from the five-carbon isoprenoid precursors isopentenyl diphosphate (IDP) and dimethylallyl diphosphate (DMADP), which are biosynthesised in nature *via* two pathways, namely the 2-methylerythritol phosphate (MEP) and the mevalonate pathways.^{2–5} The precursors of IDP and DMADP are pyruvate and D-glyceraldehyde 3-phosphate (GAP) in the MEP pathway (Fig. 1a), but solely acetyl coenzyme A in the mevalonate pathway. While mammals exclusively use the mevalonate pathway for isoprenoid biosynthesis, most eubacteria, chloroplast-containing plants and apicomplexan parasites

(including *Plasmodium falciparum*) rely on the MEP pathway.^{3–6} In the first and rate-limiting step of the MEP pathway, pyruvate and GAP are converted into 1-deoxy-D-xylulose 5-phosphate (DXP) and CO₂ by DXP synthase (DXPS), a thiamine diphosphate (ThDP)-dependent enzyme.^{5–22} This makes DXPS an attractive target for the development of anti-infectious agents and herbicides.^{5,6} Thus, there have been many studies of DXPS^{7–22} and its inhibition.^{23–33}

Clomazone (**1**), a soil-applied herbicide, is effective against grass and broadleaf weeds in many crops.³⁴ Ketoclofazone (**2a**), a metabolite of **1**, is one of the earliest reported DXPS inhibitors.^{32–34} Clomazone treatment causes bleaching of plant seedlings but to be active, it must be oxidised into **2a**. By inhibiting DXPS in the MEP pathway, **2a** suppresses isoprenoid biosynthesis in plastids and leads to impaired chloroplast development and pigment loss.^{5,6,32–34}

Further studies showed that **2a** and its ring-opened form, carboxylate **3a**, suppressed the growth of two pathogenic bacteria, *Escherichia coli* and *Haemophilus influenzae*, due to inhibition of DXPS (data summarised in Fig. 1a).^{32,33} In general, **3a** is a stronger inhibitor of DXPS but **2a** is more potent in cell-based assays.^{5,6,32–35} Presumably this is because **2a** is more hydrophobic and diffuses better through the membrane and, once inside the cell, **2a** is then hydrolysed to **3a** for stronger inhibition of DXPS.⁵ Kinetic studies revealed that the inhibitory action of **2a** on *Hi*DXPS and *Ec*DXPS is

^a Yusuf Hamied Department of Chemistry, University of Cambridge, Lensfield Road, Cambridge CB2 1EW, UK. E-mail: fjl1@cam.ac.uk^b Research School of Biology, The Australian National University, Canberra, ACT, 2601, Australia^c Helmholtz Institute for Pharmaceutical Research Saarland (HIPS) – Helmholtz Centre for Infection Research (HZI), Campus Building E8.1, 66123 Saarbrücken, Germany^d Department of Pharmacy, Saarland University, Campus Building E8.1, 66123 Saarbrücken, Germany† Electronic supplementary information (ESI) available. See DOI: <https://doi.org/10.1039/d4md00083h>

‡ Equal contribution.

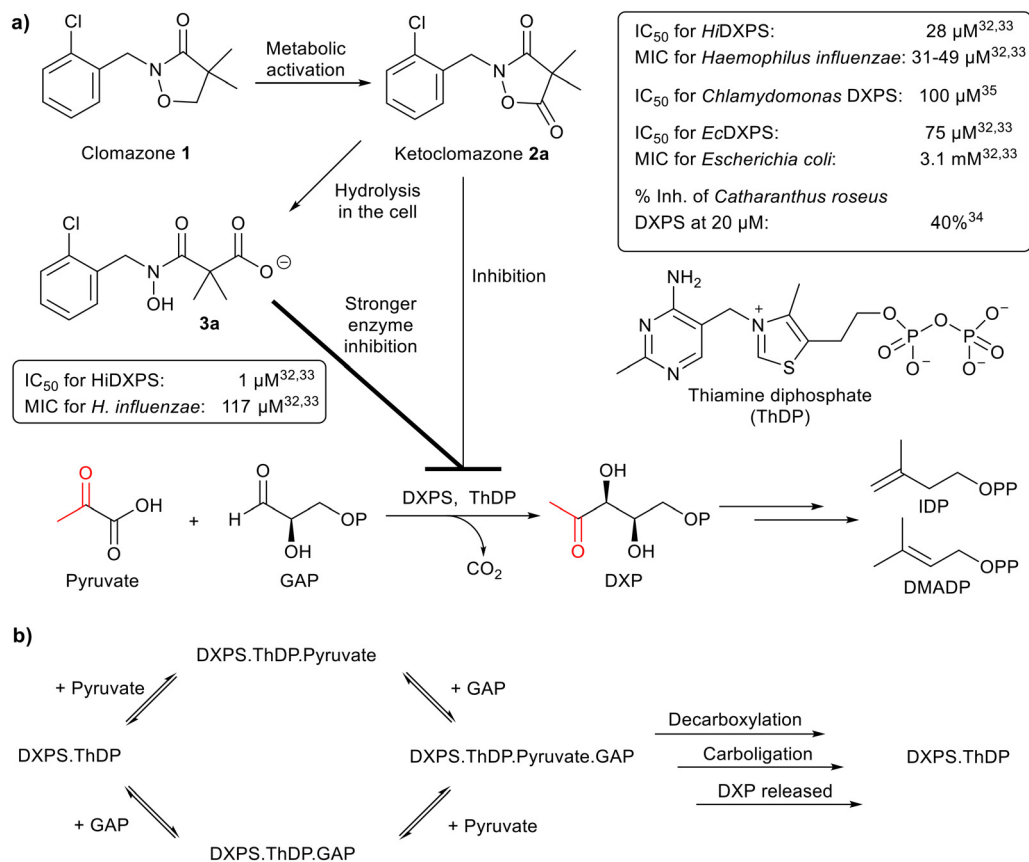
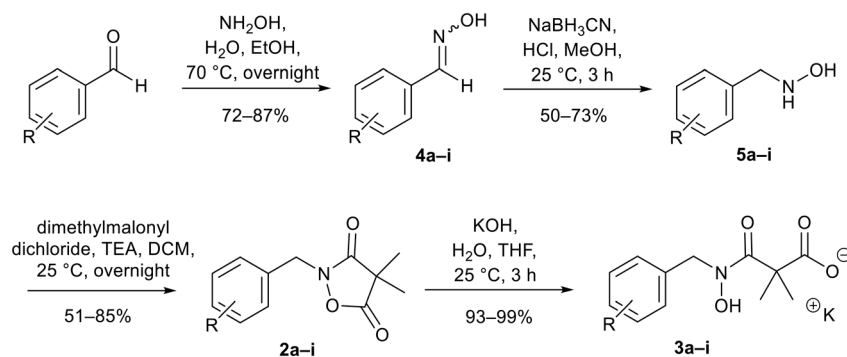


Fig. 1 a) Biochemical reaction and inhibition of DXP synthase. DXPS, catalysing the first step of the MEP pathway, is the target of **2a** and **3a**; their biological activities are summarised in the boxes. MIC, minimum inhibitory concentration. b) Random sequential mechanism of DXPS.

uncompetitive with respect to pyruvate and mixed type (close to non-competitive) with respect to GAP.^{32,33} The mode of inhibition by **3a** has yet to be determined.

In this study, we studied the activities of **2a** and **3a** against a range of ThDP-dependent enzymes, DXPS enzymes from four species and four other ThDP-dependent enzymes, namely pyruvate dehydrogenase E1-subunit (PDH E1), pyruvate decarboxylase (PDC), pyruvate oxidase (PO) and 2-oxoglutarate dehydrogenase E1-subunit (OGDH E1). Both **2a** and **3a** inhibited not only EcDXPS (consistent with the

earlier findings^{32,33}) but also PDH E1, and we determined their modes of inhibition. They showed little or no inhibition of the DXPS enzymes from the other bacteria or of the other ThDP-dependent enzymes. To further understand their inhibition, we prepared analogues **2b-i** and **3b-i** and evaluated them as inhibitors of EcDXPS and PDH E1 in biochemical and computational studies. These results may provide useful insights to facilitate further development of selective inhibitors of DXPS as anti-infectious agents and herbicides.



Scheme 1 Chemical synthesis of **2a** and **3a** and analogues. Identity of the R-groups: a: o-Cl, b: H, c: o-F, d: o-Br, e: p-Cl, f: p-F, g: p-Br, h: o-Me and i: p-tBu.



Results and discussion

Chemical synthesis of compounds 2 and 3 and analogues

Ketoclozomazone **2a** and its ring-opened form **3a** were synthesised by reported methods.³³ As shown in Scheme 1, *o*-chlorobenzaldehyde was condensed with NH_2OH to give oxime **4a**, which was reduced with NaBH_3CN under acidic conditions to give hydroxylamine **5a**. Coupling with dimethylmalonyl dichloride yielded ketoclozomazone **2a** and hydrolysis under basic conditions afforded the ring-opened form **3a**.

A decade ago, the Ohkanda group prepared three analogues of **3a** as potential antibacterial agents by modifying the acyclic side chain.³³ However, all three analogues showed greatly reduced inhibition of DXPS and suppression of the growth of *H. influenzae*.³³ Thus, in this study, we made analogues of **2a** and **3a** by modifying the aromatic ring. We chose to change the existing *o*-Cl of **2a** and **3a** to alternative substituents and we also tested some *para*-substituted analogues as this is probably the most exposed position, susceptible to metabolic oxidation. Eight analogues of each (**2b–i** and **3b–i**) were synthesised by the synthetic route in Scheme 1; among these, **2c** and **2d** were described in a patent in 1981.³⁶

Identifying inhibitory activities of compounds 2 and 3 on *Ec*DXPS and porcine PDH E1

Inhibition by **2a** and **3a** was evaluated on DXPS enzymes from four different species, namely, *Klebsiella pneumoniae*, *Pseudomonas aeruginosa*, *Deinococcus radiodurans* and *E. coli*. Both were inhibitors of *Ec*DXPS (87–92% inhibition at 1 mM), consistent with earlier reports, but they had low activity on *Kp*DXPS, *Pa*DXPS and *Dr*DXPS (<16% inhibition at 1 mM§) (Table S1†). The selectivity of **2a** and **3a** as inhibitors of DXPS over other ThDP-dependent enzymes has not yet been reported, so they were also tested against four other ThDP-dependent enzymes: they showed inhibition of porcine PDH E1 (52–71% inhibition at 100 μM) but lacked activity on PDC, PO and OGDH E1 (<5% inhibition at 250 μM).

Although apicomplexan parasites (in addition to most bacteria and plants) rely on the MEP pathway for isoprenoid biosynthesis,^{3–6} only antibacterial and herbicidal activities of ketoclozomazone **2a** and its ring-opened form **3a** have been reported. *Pf*DXPS was not available, so the antiparasitic activities of **2a** and **3a** were assessed by determining their effects on *in vitro* proliferation of the 3D7 strain of *P. falciparum*. Infected red blood cells were treated with **2a** and **3a**, and parasite proliferation was measured by performing SYBR-Safe assay, which correlates fluorescence intensity to parasite DNA.^{37–39} Unfortunately, both compounds showed minimal antiparasitic activities even at high-micromolar levels (Fig. S1†). Given that fosmidomycin, which targets the second enzyme in the MEP pathway, has potent antimalarial activity,⁴⁰

this negative result led us to suspect that, as with *Kp*DXPS, *Pa*DXPS and *Dr*DXPS, **2a** and **3a** may not be good inhibitors of *Pf*DXPS, despite assumptions to the contrary.⁴¹

Kinetic studies of *Ec*DXPS inhibition

The Kuzuyama group studied the inhibition of *Ec*DXPS by ketoclozomazone **2a** in 2010.³² In their assays, conducted in Tris buffer, DXPS seemed to follow a ping-pong bi-bi mechanism (as is normal for ThDP-dependent enzymes⁴²) in which pyruvate reacts with the ThDP-bound DXPS and is decarboxylated and then GAP binds and reacts with the resultant intermediate to yield the DXP product.³² K_{M} values of pyruvate and GAP were 48 and 370 μM , respectively. **2a** was found to be uncompetitive with respect to pyruvate (with $K_{\text{I}}^{\text{pyruvate}} = 75 \mu\text{M}$) and mixed-type with respect to GAP (with $K_{\text{I}}^{\text{GAP}} = 220\text{--}460 \mu\text{M}$).³² More recent studies, using different buffers, demonstrated that both pyruvate and GAP can bind to the free enzyme (DXPS·ThDP in Fig. 1b), arguing against a strictly ordered mechanism, and a random sequential mechanism has been proposed for *Ec*DXPS^{8,25} and several other bacterial and protozoan DXPS enzymes, including *P. falciparum*¹² and *D. radiodurans*.^{16–18} A buffer-optimisation study conducted by the Freil Meyers group showed that $K_{\text{M}}^{\text{GAP}}$ values increased with the Tris concentration and they attributed this to the reactivity of the aldehyde group of GAP towards the amino group of Tris.⁸ Conducting *Ec*DXPS assays in HEPES buffer, they found improved reactivity with $K_{\text{M}}^{\text{pyruvate}} = 49 \mu\text{M}$ and $K_{\text{M}}^{\text{GAP}} = 24 \mu\text{M}$.⁸ In our work, using the same buffer, we obtained very similar K_{M} values for pyruvate and GAP of 50 and 25 μM , respectively (Fig. S2†). With the more recent findings on the mechanism and the improved assay conditions, we aimed to re-examine the interactions between ketoclozomazone (**2a**) and *Ec*DXPS and extend the kinetic studies to inhibition by **3a** and by analogues of both **2a** and **3a**.

Inhibition of *Ec*DXPS by **2a** and **3a** in HEPES buffer was evaluated in kinetic studies. As Fig. 2 shows, inhibition by **2a** is uncompetitive with respect to pyruvate and mixed (approximately non-competitive) with respect to GAP, with $K_{\text{I}}^{\text{pyruvate}}$ measured to be 84 μM at high [GAP] (250 $\mu\text{M} = 10 K_{\text{M}}$). Our findings on **2a** were mostly consistent with those from the Kuzuyama group,³² except our $K_{\text{I}}^{\text{GAP}}$ at high [pyruvate] (1 mM = 20 K_{M}) was *ca.* 6 μM compared to their 220–460 μM . This much lower $K_{\text{I}}^{\text{GAP}}$ value is presumably due to the different assay conditions used (HEPES buffer and higher [pyruvate]) and is consistent with the much lower $K_{\text{M}}^{\text{GAP}}$ in this buffer. The inhibition by **3a** was found to be uncompetitive with respect to both pyruvate and GAP, with K_{I} values of 5 and 9 μM , respectively (Fig. 2). The shift in inhibition modality with respect to GAP from non-competitive (**2a**) to uncompetitive (**3a**), though unexpected, is reasonable given their structural differences.

We then studied how the substitution pattern of the aromatic scaffold affects the inhibition of *Ec*DXPS. The

§ *Kp*DXPS was assayed at 10 mM of inhibitor and showed 64% inhibition by **2a** but calculation suggests this would equate to <16% inhibition at 1 mM.



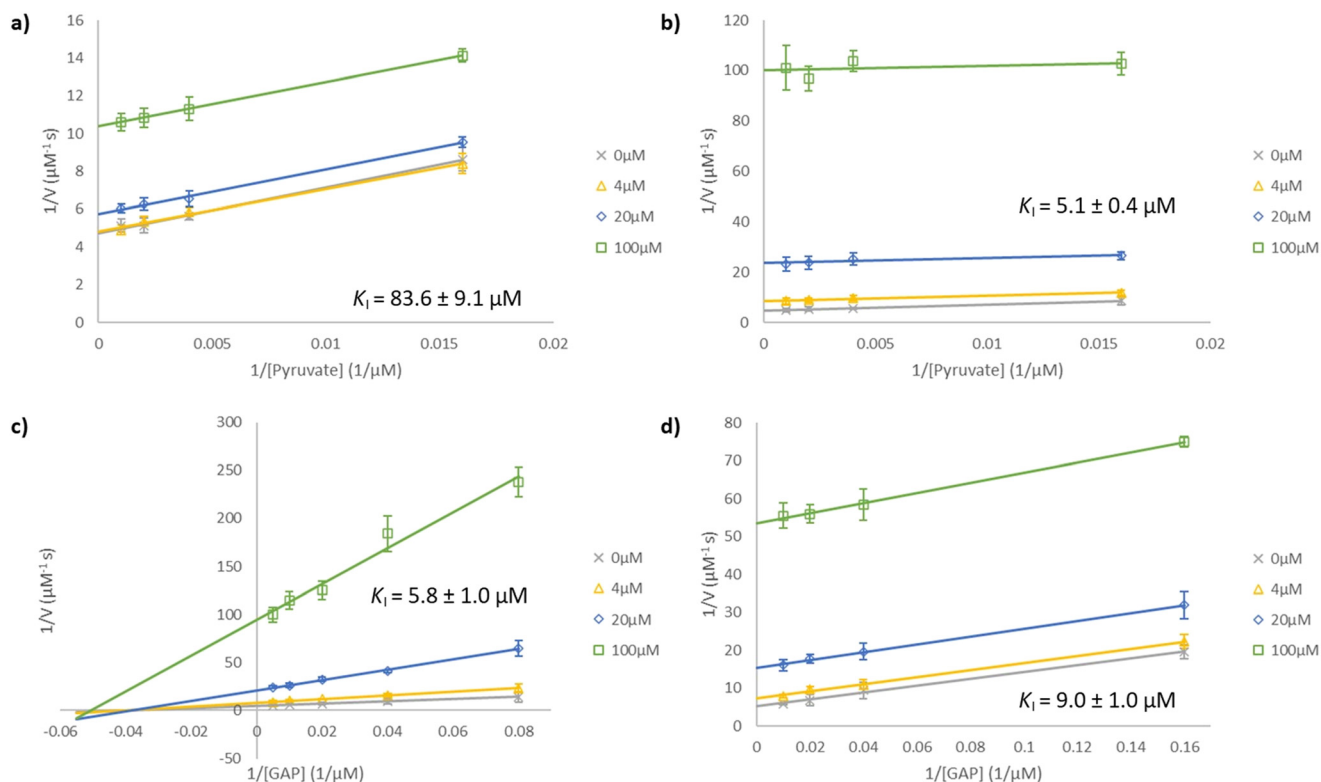


Fig. 2 Lineweaver-Burk plots for *EcDXPS* inhibition. Compounds were assayed at concentrations of 0 μM (\times), 4 μM (Δ), 20 μM (\diamond) and 100 μM (\square). Inhibition by (a) **2a** and (b) **3a** at a fixed [GAP] of 250 μM ($10 K_M$) under varying [pyruvate] of 62.5, 250, 500 and 1000 μM . Inhibition by (c) **2a** and (d) **3a** at a fixed [pyruvate] of 1 mM ($20 K_M$) under varying [GAP] of 12.5, 25, 50, 100 and 200 μM and 6.25, 25, 50 and 100 μM respectively. The lines in plot (a), (b) and (d) are essentially parallel, indicating uncompetitive inhibition, while the lines in plot (c) intersect approximately on the x-axis (mixed or non-competitive inhibition).

percentage inhibition was measured for compounds at 5 μM under different concentrations of pyruvate and GAP: pyruvate was fixed at either 62.5 μM ($= 1.25 K_M$, shown as [P]) or 1 mM ($= 20 K_M$, shown as [P]) while GAP was fixed at either 50 μM ($= 2 K_M$, shown as [G]) or 250 μM ($= 10 K_M$, shown as [G]) (Table 1). The inhibitory activities of analogues **2b-f**

increased (from 17–27% to 37–48%) with [pyruvate] but did not change with [GAP], consistent with the mode of inhibition by **2a**, *i.e.* uncompetitive with respect to pyruvate and non-competitive with respect to GAP. The inhibitory activities of analogues **3b-d** increased with both [pyruvate] and [GAP], consistent with the modality of inhibition by **3a**,

Table 1 Summary of inhibitory activity on *EcDXPS*

Compound	Inhibition ^a (%)				Compound	Inhibition ^a (%)			
	[P], [G]	[P], [G]	[P], [G]	[P], [G]		[P], [G]	[P], [G]	[P], [G]	[P], [G]
2a (<i>o</i> -Cl)	24 \pm 3	48 \pm 2	21 \pm 3	47 \pm 3	3a (<i>o</i> -Cl)	26 \pm 2	55 \pm 5	48 \pm 3	65 \pm 5
2b (H)	20 \pm 3	37 \pm 3	21 \pm 2	39 \pm 2	3b (H)	26 \pm 3	46 \pm 5	38 \pm 3	53 \pm 3
2c (<i>o</i> -F)	22 \pm 2	48 \pm 3	22 \pm 3	44 \pm 4	3c (<i>o</i> -F)	19 \pm 2	52 \pm 3	30 \pm 2	55 \pm 2
2d (<i>o</i> -Br)	27 \pm 2	40 \pm 4	27 \pm 3	39 \pm 4	3d (<i>o</i> -Br)	30 \pm 2	48 \pm 3	37 \pm 3	51 \pm 4
2e (<i>p</i> -Cl)	19 \pm 2	42 \pm 3	20 \pm 4	42 \pm 2	3e (<i>p</i> -Cl)	14 \pm 3	49 \pm 2	24 \pm 3	23 \pm 2
2f (<i>p</i> -F)	17 \pm 3	37 \pm 3	18 \pm 2	40 \pm 4	3f (<i>p</i> -F)	17 \pm 3	41 \pm 3	28 \pm 3	24 \pm 2
2g (<i>p</i> -Br)	8 \pm 2	43 \pm 4	19 \pm 3	17 \pm 4	3g (<i>p</i> -Br)	14 \pm 2	44 \pm 2	24 \pm 3	21 \pm 4
2h (<i>o</i> -Me)	12 \pm 2	37 \pm 3	21 \pm 3	22 \pm 2	3h (<i>o</i> -Me)	17 \pm 3	39 \pm 4	23 \pm 2	21 \pm 2
2i (<i>p</i> - ^{<i>t</i>} Bu)	7 \pm 2	39 \pm 3	15 \pm 2	15 \pm 3	3i (<i>p</i> - ^{<i>t</i>} Bu)	8 \pm 3	39 \pm 4	18 \pm 2	16 \pm 3

^a Data are the means of measurements in three technical replicates. Percentage inhibition values were determined for compounds at 5 μM with [pyruvate] = 62.5 μM ([P]) or 1 mM ([P]) and [GAP] = 50 μM ([G]) or 250 μM ([G]).

i.e. uncompetitive with respect to both pyruvate and GAP. Based on these findings, we speculate that the inhibitory mechanism of ketoclozazone **2a** (and **2b–f**) is as follows (Fig. 1b): prior to the entry of pyruvate, the inhibitors barely bind to either the DXPS·ThDP free enzyme or the DXPS·ThDP·GAP complex. When pyruvate binds it induces a conformational change in an unidentified inhibitor site (likely to be different from the substrate-binding sites), **2** can then engage the enzyme (with comparable inhibition of both the DXPS·ThDP·pyruvate and the DXPS·ThDP·pyruvate·GAP complexes). In the case of **3a** (and **3b–d**), it can only engage the enzyme when both substrates are bound as it is uncompetitive towards both, and it exhibits the strongest inhibition when both substrates are bound.

Analogues **2g–i** and **3e–i** showed the weakest inhibition (7–17%) under low level of both substrates, improved inhibition (15–28%) under high [GAP], and the strongest inhibition (37–49%) under high [pyruvate] but low [GAP]; such a change in the inhibition profile may have a steric origin as they are all larger than **2a** and **3a**. As a result, we did not explore any larger substituents in the *ortho*- or *para*-positions. Although none of the *para*-substituted analogues had improved inhibition relative to the unsubstituted **2a**, it is worth noting that **2e** and **2f** (*p*-Cl and *p*-F) have similar activities to **2a**. So, if metabolic oxidation at the *para*-position does prove to be a problem, these substituents (in addition to the *o*-Cl) may well provide a solution. While the binding location of **2a** and **3a** is unknown, with no available crystal structures of them bound to EcDXPS, we believe that their binding sites are likely to be distinct due to their different inhibition modalities. As these inhibitor sites are highly sensitive to structural modifications on ligands and they are probably not in the active site, this may help to explain why **2a** and **3a** bind poorly to several other DXPS enzymes.

Kinetic studies on porcine PDH E1 inhibition

In the preliminary screening on multiple ThDP-dependent enzymes (Table S1†), inhibition of porcine PDH E1 by **2a** and **3a** was discovered. To gain insights into their binding mode, computational docking was performed: both were predicted to occupy the coenzyme-binding site (Fig. 3). Their competitive relationship with ThDP was confirmed

experimentally as the observed potency decreased with increasing [ThDP] (Table 2). With the IC₅₀ values of their dose-dependent inhibition determined (Fig. S3†), the affinities of **2a** and **3a** were found to be comparable to and 2.5 times weaker than that of ThDP, respectively; as the *K_M* value for ThDP is 50 nM,³¹ this puts their *K_i* values in the nanomolar range (*K_i* of **2a** = 44 nM and *K_i* of **3a** = 127 nM).

The analogues were also tested, to probe the structure–activity relationship (SAR). The ring-opened **3a–h** (13–59%) were consistently weaker inhibitors than the cyclic **2a–h** (37–79%) at 100 μM with [ThDP] = 25 μM (Table 2). This supports a binding mode in which the non-aromatic ring of our inhibitors occupies the central hydrophobic region (Fig. 3). The charged ring-opened series would suffer a greater desolvation penalty than the cyclic series upon leaving the aqueous environment and binding in this hydrophobic region.^{31,43–46} If the highly polar moiety of the ring-opened series were able to interact with the Mg²⁺ ion in the diphosphate pocket, they would be expected to bind better than the cyclic series, so we suggest that the side chain is not long enough to allow any effective interaction with the Mg²⁺ ion.

Regarding the substitution pattern on the aromatic ring of our inhibitors, the position and identity of the halogen atom (F or Cl) does not seem to affect affinity (compared to the unsubstituted **2b** and **3b**), but the bromo compounds were weaker binders. For alkyl substituents, having a Me- on the *ortho*-position reduced affinity while introducing a *t*Bu group on the *para*-position abolished binding, presumably for steric reasons. These trends were consistent in both series (Table 2). Our docking models suggested that this *para*-substituent of our inhibitors occupies the same space as the methyl group on the aminopyrimidine ring of ThDP when bound to the enzyme (Fig. 3), and this is supported by the low activity of **2i** and **3i**: our earlier work⁴⁴ on developing PDH-selective inhibitors showed that substituents larger than a methyl group at this *para*-position led to poor binding. So the predicted binding modes in this study were in line with our understanding of PDH E1's ThDP-binding site.

Further evaluation – cytotoxicity and membrane-permeability

Regardless of their precise binding modes, **2a** and **3a** were found to be potent inhibitors of PDH E1. Ligand efficiency

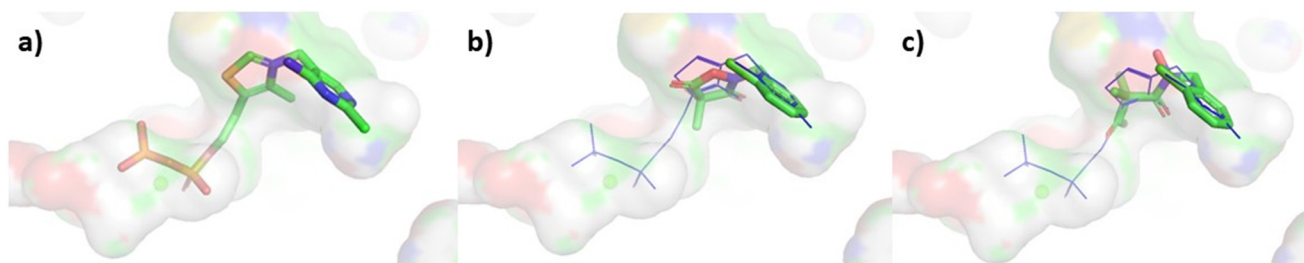
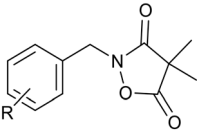
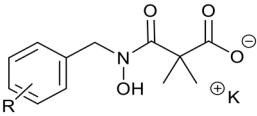


Fig. 3 (a) Binding mode of ThDP in PDH E1 showing the V-shaped conformation between the aminopyrimidine and the thiazolium ring. The thiazolium ring is in a relatively hydrophobic region, which facilitates formation of the catalytic ylide. Predicted binding modes of **2a** (b) and **3a** (c) overlaid with ThDP (blue wires) as in view (a). Molecules were generated using Mercury and dockings were executed using GOLD docking programme with human PDH (PDB: 6CFO) as the target; the reported modelling procedures⁴² have been adopted in this study.



Table 2 Summary of inhibitory activity on porcine PDH E1

							
Inhibition ^a (%)				Inhibition ^a (%)			
[Compound]:[ThDP]				[Compound]:[ThDP]			
Compounds	4 : 1	1 : 1	1 : 4	Compounds	4 : 1	1 : 1	1 : 4
2a (<i>o</i> -Cl)	75 ± 5	53 ± 3	25 ± 4	3a (<i>o</i> -Cl)	55 ± 3	32 ± 3	8 ± 3
2b (H)	78 ± 4	54 ± 2	29 ± 2	3b (H)	59 ± 3	31 ± 2	9 ± 2
2c (<i>o</i> -F)	74 ± 4	51 ± 3	22 ± 2	3c (<i>o</i> -F)	55 ± 4	29 ± 4	<5
2d (<i>o</i> -Br)	39 ± 6	18 ± 4	<5	3d (<i>o</i> -Br)	17 ± 3	<5	<5
2e (<i>p</i> -Cl)	79 ± 4	57 ± 3	19 ± 4	3e (<i>p</i> -Cl)	58 ± 2	37 ± 3	<5
2f (<i>p</i> -F)	73 ± 4	44 ± 3	13 ± 3	3f (<i>p</i> -F)	55 ± 4	23 ± 4	<5
2g (<i>p</i> -Br)	37 ± 5	14 ± 4	<5	3g (<i>p</i> -Br)	13 ± 4	<5	<5
2h (<i>o</i> -Me)	37 ± 4	16 ± 3	<5	3h (<i>o</i> -Me)	14 ± 3	<5	<5
2i (<i>p</i> - ^t Bu)	<5	<5	<5	3i (<i>p</i> - ^t Bu)	<5	<5	<5

^a Data are the means of measurements in three technical replicates. Percentage inhibition values were determined for compounds at 100 μM with [ThDP] = 25 μM (for 4 : 1); at 100 μM with [ThDP] = 100 μM (for 1 : 1); at 25 μM with [ThDP] = 100 μM (for 1 : 4).

(LE), measuring the binding energy to its target (in kcal mol⁻¹) per heavy atom of the ligand is a widely applied metric in medicinal chemistry;⁴⁷ drug-discovery efforts often aim to develop clinical candidates with LE > 0.3.^{47,48} As the LEs of **2a** and **3a** are 0.61 (binding energy = 10.4 kcal mol⁻¹; heavy atom count = 17) and 0.54 (binding energy = 9.8 kcal mol⁻¹; heavy atom count = 18), respectively, both are highly efficient inhibitors of PDH E1.

Given that the PDH complex provides a link between glycolysis and mitochondrial metabolism for energy production,⁴⁹ concern was raised over possible cytotoxicity due to PDH inhibition. To test this, human foreskin fibroblast (HFF) cells were subjected to compounds **2a** and **3a**, and the compounds were only weakly cytotoxic, even at concentrations 100 times greater than their *K*_i values (Fig. S4†). Although one possible explanation would be that **2a** and **3a** are weak inhibitors of human PDH E1 despite their potent inhibition on porcine PDH E1, it is generally accepted that the latter is a good model for the former because the sequence of the two enzymes are >95% identical and the residues that differ are located away from the active site.⁴⁴ Another possible explanation would be due to hydrolysis of **2a** into **3a**.²⁵ Extracellular hydrolysis would lead to reduced cell entry of inhibitors as **3a** is almost membrane-impermeable (fraction absorbed = 6% in parallel artificial membrane permeability assay, PAMPA,⁵⁰ as shown in Table S2†). Intracellular hydrolysis would lead to reduced entry into the mitochondria, which is where the PDH complex is active.⁴⁹ And in either case inhibition of PDH would be lowered as **3a** is a less potent inhibitor than **2a**.

Given the inhibitory activity on *Ec*DXPS and the lack of cytotoxicity on HFF cells, the potential of ketoclozazone **2a** as an antibacterial agent against susceptible bacteria is enhanced. Previous studies had already established its

micromolar activities on suppressing bacterial cell growth,^{32,33} in addition to its herbicidal action. This study provides additional insight into its antibacterial potential. The cyclic form **2a** probably serves as a prodrug that facilitates membrane permeability (fraction absorbed = 47% in PAMPA, Table S2†); once inside the cell, it gets hydrolysed to its ring-opened form **3a**, which has several important biological consequences: a) this charged form may be trapped within the cells, thus raising the intracellular inhibitor level; b) **3a** is a weaker inhibitor of PDH than its parent **2a**, thus likely to be less cytotoxic to human cells; and c) although **2a** and **3a** are both potent inhibitors of DXPS, the shift in inhibition modality with respect to GAP from non-competitive (**2a**) to uncompetitive (**3a**) makes the latter a better anti-infectious agent. This is because when an enzyme in a metabolic pathway is inhibited, the upstream metabolic processes continue to make new substrates and this will lead to a build-up of the substrates for that enzyme. As the substrate concentration continues to rise, it is likely to eventually exceed the *K*_M value and approach saturating conditions. This will lead to a relief of inhibition by competitive inhibitors but an increase in the affinity of uncompetitive inhibitors; in the latter case, further suppression of the metabolic pathway could eventually be catastrophic to cells.⁵¹ Our biological data may help put these into context. Equimolar concentrations of **2a** and ThDP leads to 53% inhibition of PDH E1 activity; if **2a** gets hydrolysed to **3a** and the cell increases the ThDP content by four-fold, the percentage inhibition would drop to 8% (Table 2). By contrast, the percentage inhibition of DXPS is 24% for **2a** at 5 μM with [pyruvate] and [GAP] close to their respective *K*_M values; when hydrolysis occurs and, if the substrates accumulate upon DXPS inhibition to the higher levels used in Table 1, the percentage inhibition would rise to 65%.



Conclusions

Clomazone **1** is a soil-applied herbicide, and ketoclozomazone **2a** is believed to be the active species. It has also been showed that **2a** can be an antibacterial agent and that **2a** and **3a** probably suppress bacterial growth through inhibition of DXPS.^{32–34} This study revisited compounds **2a** and **3a** as inhibitors of a range of DXPS enzymes and also evaluated their activities on the broader ThDP-dependent enzyme family. Among the four tested DXPS enzymes, **2a** and **3a** only potently inhibited *Ec*DXPS. The kinetics of inhibition of **2a** was shown to be uncompetitive with respect to pyruvate and non-competitive with respect to GAP, while that of **3a** was found to be uncompetitive with respect to both substrates. Screened on four other ThDP-dependent enzymes, **2a** and **3a** were identified as ThDP-competitive inhibitors of porcine PDH E1. Despite this, however, **2a** and **3a** showed little cytotoxicity towards human cells, probably because of hydrolysis of **2a** to **3a**, which is relatively impermeable towards membranes. Our findings and those of others suggest that the more hydrophobic **2a** acts as a prodrug for membrane passage and gets hydrolysed to **3a** in cells.^{5,6,32,33} The differences in inhibitory activities and modalities on the DXPS and PDH enzymes between **2a** and **3a**, established in this study, support the potential of ketoclozomazone **2a** as a selective antibacterial agent. This study expands our understanding on ketoclozomazone as an inhibitor of the ThDP-dependent enzyme family and may aid work on the development of DXPS inhibitors.

Author contributions

AHYC performed the chemical synthesis. TCSH performed the computational studies. IF performed the cell-based assays. AHYC, TCSH and RH performed the enzyme assays. AHYC and TCSH wrote the first draft. FJL supervised the work from AHYC and TCSH. KJS supervised the work from IF. AKHH supervised the work from RH. All authors edited a draft of the manuscript and approved the final version.

Conflicts of interest

The authors declare no competing financial interest.

Acknowledgements

We are grateful for the support from K. M. Medhealth (AHYC and TCSH), Research Training Program scholarship from the Australian government (IF), the Canberra Branch of the Australian Red Cross Lifeblood for the provision of red blood cells, members of the van Dooren Lab (Australian National University) for HFF cells, the Schlumberger Foundation Faculty for the Future Fellowship (RH) and the Helmholtz Association Initiative and Networking Fund and the European Research Council, ERC starting grant 757913 (AKHH).

References

- S. D. Tetali, Terpenes and isoprenoids: a wealth of compounds for global use, *Planta*, 2019, **249**, 1–8, DOI: [10.1007/s00425-018-3056-x](https://doi.org/10.1007/s00425-018-3056-x).
- K. Bloch, Sterol molecule: structure, biosynthesis, and function, *Steroids*, 1992, **57**, 378–383, DOI: [10.1016/0039-128x\(92\)90081-j](https://doi.org/10.1016/0039-128x(92)90081-j).
- T. Kuzuyama and H. Seto, Diversity of the biosynthesis of the isoprene units, *Nat. Prod. Rep.*, 2003, **20**, 171–183, DOI: [10.1039/B109860H](https://doi.org/10.1039/B109860H).
- S. Heuston, M. Begley, C. G. M. Gahan and C. Hill, Isoprenoid biosynthesis in bacterial pathogens, *Microbiology*, 2012, **158**, 1389–1401, DOI: [10.1099/mic.0.051599-0](https://doi.org/10.1099/mic.0.051599-0).
- A. A. DeColli, M. L. Johnston and C. L. Freel Meyers, Recent Insights into Mechanism and Structure of MEP Pathway Enzymes and Implications for Inhibition Strategies, in *Comprehensive Natural Products III*, ed. H.-W. Liu and T. P. Begley, Elsevier, 2020, vol. 4, pp. 287–322.
- D. Bartee and C. L. Freel Meyers, Toward Understanding the Chemistry and Biology of 1-Deoxy-d-xylulose 5-Phosphate (DXP) Synthase: A Unique Antimicrobial Target at the Heart of Bacterial Metabolism, *Acc. Chem. Res.*, 2018, **51**, 2546–2555, DOI: [10.1021/acs.accounts.8b00321](https://doi.org/10.1021/acs.accounts.8b00321).
- L. A. Brammer and C. Freel Meyers, Revealing Substrate Promiscuity of 1-Deoxy-D-xylulose 5-Phosphate Synthase, *Org. Lett.*, 2009, **11**, 4748–4751, DOI: [10.1021/ol901961q](https://doi.org/10.1021/ol901961q).
- L. A. Brammer, J. M. Smith, H. Wade and C. Freel Meyers, 1-Deoxy-D-xylulose 5-Phosphate Synthase Catalyzes a Novel Random Sequential Mechanism, *J. Biol. Chem.*, 2011, **286**, 36522–36531, DOI: [10.1074/jbc.M111.259747](https://doi.org/10.1074/jbc.M111.259747).
- H. Patel, N. S. Nemeria, L. A. Brammer, C. L. Freel Meyers and F. Jordan, Observation of Thiamin-Bound Intermediates and Microscopic Rate Constants for Their Interconversion on 1-Deoxy-d-xylulose 5-Phosphate Synthase: 600-Fold Rate Acceleration of Pyruvate Decarboxylation by D-Glyceraldehyde-3-phosphate, *J. Am. Chem. Soc.*, 2012, **134**, 18374–18379, DOI: [10.1021/ja307315u](https://doi.org/10.1021/ja307315u).
- S. Handa, D. Ramamoorthy, T. J. Spradling, W. C. Guida, J. H. Adams, K. G. Bendinskas and D. J. Merkler, Production of recombinant 1-deoxy-d-xylulose-5-phosphate synthase from *Plasmodium vivax* in *Escherichia coli*, *FEBS Open Bio*, 2013, **3**, 124–129, DOI: [10.1016/j.fob.2013.01.007](https://doi.org/10.1016/j.fob.2013.01.007).
- D. Ramamoorthy, S. Handa, D. J. Merkler and W. C. Guida, *Plasmodium vivax* 1-deoxy-D-xylulose-5-phosphate synthase: Homology Modeling, Domain Swapping, and Virtual Screening, *J. Data Min. Genomics Proteomics*, 2014, **S1**, 003, DOI: [10.4172/2153-0602.S1-003](https://doi.org/10.4172/2153-0602.S1-003).
- M. R. Battistini, C. Shoji, S. Handa, L. Breydo and D. J. Merkler, Mechanistic binding insights for 1-deoxy-D-xylulose-5-phosphate synthase, the enzyme catalyzing the first reaction of isoprenoid biosynthesis in the malaria-causing protists, *Plasmodium falciparum* and *Plasmodium vivax*, *Protein Expression Purif.*, 2016, **120**, 16–27, DOI: [10.1016/j.pep.2015.12.003](https://doi.org/10.1016/j.pep.2015.12.003).



- 13 J. K. White, S. Handa, S. L. Vankayala, D. J. Merkler and H. L. Woodcock, Thiamin Diphosphate Activation in 1-Deoxy-d-xylulose 5-Phosphate Synthase: Insights into the Mechanism and Underlying Intermolecular Interactions, *J. Phys. Chem. B*, 2016, **120**, 9922–9934, DOI: [10.1021/acs.jpcc.6b07248](#).
- 14 D. Bartee and C. L. Freel Meyers, Targeting the Unique Mechanism of Bacterial 1-Deoxy-d-xylulose-5-phosphate Synthase, *Biochemistry*, 2018, **57**, 4349–4356, DOI: [10.1021/acs.biochem.8b00548](#).
- 15 A. A. DeColli, N. S. Nemeria, A. Majumdar, G. J. Gerfen, F. Jordan and C. L. Freel Meyers, Oxidative decarboxylation of pyruvate by 1-deoxy-d-xylulose 5-phosphate synthase, a central metabolic enzyme in bacteria, *J. Biol. Chem.*, 2018, **293**, 10857–10869, DOI: [10.1074/jbc.ra118.001980](#).
- 16 S. Handa, D. R. Dempsey, D. Ramamoorthy, N. Cook, W. C. Guida, T. J. Spradling, J. K. White, H. L. Woodcock and D. J. Merkler, Mechanistic Studies of 1-Deoxy-D-Xylulose-5-Phosphate Synthase from *Deinococcus radiodurans*, *Biochem. Mol. Biol. J.*, 2018, **4**(1), 2, DOI: [10.21767/2471-8084.100051](#).
- 17 P. Y.-T. Chen, A. A. DeColli, C. L. Freel Meyers and C. L. Drennan, X-ray crystallography-based structural elucidation of enzyme-bound intermediates along the 1-deoxy-d-xylulose 5-phosphate synthase reaction coordinate, *J. Biol. Chem.*, 2019, **294**, 12405–12414, DOI: [10.1074/jbc.ra119.009321](#).
- 18 A. A. DeColli, X. Zhang, K. L. Heflin, F. Jordan and C. L. Freel Meyers, Active Site Histidines Link Conformational Dynamics with Catalysis on Anti-Infective Target 1-Deoxy-d-xylulose 5-Phosphate Synthase, *Biochemistry*, 2019, **58**, 4970–4982, DOI: [10.1021/acs.biochem.9b00878](#).
- 19 R. M. Gierse, E. R. Reddem, A. Alhayek, D. Baitinger, Z. Hamid, H. Jakobi, B. Laber, G. Lange, A. K. H. Hirsch and M. R. Groves, Identification of a 1-deoxy-D-xylulose-5-phosphate synthase (DXS) mutant with improved crystallographic properties, *Biochem. Biophys. Res. Commun.*, 2021, **539**, 42–47, DOI: [10.1016/j.bbrc.2020.12.069](#).
- 20 M. L. Johnston and C. L. Freel Meyers, Revealing Donor Substrate-Dependent Mechanistic Control on DXPS, an Enzyme in Bacterial Central Metabolism, *Biochemistry*, 2021, **60**, 929–939, DOI: [10.1021/acs.biochem.1c00019](#).
- 21 R. M. Gierse, R. Oerlemans, E. R. Reddem, V. O. Gawriljuk, A. Alhayek, D. Baitinger, H. Jakobi, B. Laber, G. Lange, A. K. H. Hirsch and M. R. Groves, First crystal structures of 1-deoxy-D-xylulose 5-phosphate synthase (DXPS) from *Mycobacterium tuberculosis* indicate a distinct mechanism of intermediate stabilization, *Sci. Rep.*, 2022, **12**, 7221, DOI: [10.1038/s41598-022-11205-9](#).
- 22 R. Hamid, S. Adam, A. Lacour, L. M. Gomez, J. Köhnke and A. K. H. Hirsch, 1-deoxy-D-xylulose-5-phosphate synthase from *Pseudomonas aeruginosa* and *Klebsiella pneumoniae* reveals conformational changes upon cofactor binding, *J. Biol. Chem.*, 2023, **299**, 105152, DOI: [10.1016/j.jbc.2023.105152](#).
- 23 J. M. Smith, R. J. Vierling and C. Freel Meyers, Selective inhibition of *E. coli* 1-deoxy-d-xylulose-5-phosphate synthase by acetylphosphonates, *Med. Chem. Commun.*, 2012, **3**, 65–67, DOI: [10.1039/C1MD00233C](#).
- 24 F. Morris, R. Vierling, L. Boucher, J. Bosch and C. L. Freel Meyers, DXP synthase-catalyzed C-N bond formation: Nitroso substrate specificity studies guide selective inhibitor design, *ChemBioChem*, 2013, **14**, 1309–1315, DOI: [10.1002/cbic.201300187](#).
- 25 S. Sanders, R. J. Vierling, D. Bartee, A. A. DeColli, M. J. Harrison, J. L. Aklinski, A. T. Koppisch and C. L. Freel Meyers, Challenges and Hallmarks of Establishing Alkylacetylphosphonates as Probes of Bacterial 1-Deoxy-d-xylulose 5-Phosphate Synthase, *ACS Infect. Dis.*, 2017, **3**, 467–478, DOI: [10.1021/acsinfecdis.6b00168](#).
- 26 S. Sanders, D. Bartee, M. J. Harrison, P. D. Phillips, A. T. Koppisch and C. L. Freel Meyers, Growth medium-dependent antimicrobial activity of early stage MEP pathway inhibitors, *PLoS One*, 2018, **13**, e0197638, DOI: [10.1371/journal.pone.0197638](#).
- 27 D. Bartee, S. Sanders, P. D. Phillips, M. J. Harrison, A. T. Koppisch and C. L. Freel Meyers, Enamide Prodrugs of Acetyl Phosphonate Deoxy-d-xylulose-5-phosphate Synthase Inhibitors as Potent Antibacterial Agents, *ACS Infect. Dis.*, 2019, **5**, 406–417, DOI: [10.1021/acsinfecdis.8b00307](#).
- 28 R. P. Jumde, M. Guardigni, R. M. Gierse, A. Alhayek, D. Zhu, Z. Hamid, S. Johannsen, W. A. M. Elgaher, P. J. Neusens, C. Nehls, J. Haupenthal, N. Reiling and A. K. H. Hirsch, Hit-optimization using target-directed dynamic combinatorial chemistry: development of inhibitors of the anti-infective target 1-deoxy-d-xylulose-5-phosphate synthase, *Chem. Sci.*, 2021, **12**, 7775–7785, DOI: [10.1039/D1SC00330E](#).
- 29 D. Zhu, S. Johannsen, T. Masini, C. Simonin, J. Haupenthal, B. Illarionov, A. Andreas, M. Awale, R. M. Gierse, T. van der Laan, R. van der Vlag, R. Nasti, M. Poizat, E. Buhler, N. Reiling, R. Müller, M. Fischer, J.-L. Reymond and A. K. H. Hirsch, Discovery of novel drug-like antitubercular hits targeting the MEP pathway enzyme DXPS by strategic application of ligand-based virtual screening, *Chem. Sci.*, 2022, **13**, 10686–10698, DOI: [10.1039/D2SC02371G](#).
- 30 S. Johannsen, R. M. Gierse, A. Olshanova, E. Smerznak, C. Laggner, L. Eschweiler, Z. Adeli, R. Hamid, A. Alhayek, N. Reiling, J. Haupenthal and A. K. H. Hirsch, Not Every Hit-Identification Technique Works on 1-Deoxy-d-Xylulose 5-Phosphate Synthase (DXPS): Making the Most of a Virtual Screening Campaign, *ChemMedChem*, 2023, **18**, e202200590, DOI: [10.1002/cmdc.202200590](#).
- 31 A. H. Y. Chan, T. C. S. Ho, R. Irfan, R. A. A. Hamid, E. S. Rudge, A. Iqbal, A. Turner, A. K. H. Hirsch and F. J. Leeper, Design of thiamine analogues for inhibition of thiamine diphosphate (ThDP)-dependent enzymes: Systematic investigation through Scaffold-Hopping and C2-Functionalisation, *Bioorg. Chem.*, 2023, **138**, 106602, DOI: [10.1016/j.bioorg.2023.106602](#).
- 32 Y. Matsue, H. Mizuno, T. Tomita, T. Asami, M. Nishiyama and T. Kuzuyama, The herbicide ketoclozazole inhibits 1-deoxy-D-xylulose 5-phosphate synthase in the 2-C-methyl-D-erythritol 4-phosphate pathway and shows antibacterial



- activity against *Haemophilus influenzae*, *J. Antibiot.*, 2010, **63**, 583–588, DOI: [10.1038/ja.2010.100](#).
- 33 D. Hayashi, N. Kato, T. Kuzuyama, Y. Sato and J. Ohkanda, Antimicrobial N-(2-chlorobenzyl)-substituted hydroxamate is an inhibitor of 1-deoxy-d-xylulose 5-phosphate synthase, *Chem. Commun.*, 2013, **49**, 5535–5537, DOI: [10.1039/C3CC40758F](#).
 - 34 Y. Ferhatoglu and M. Barrett, Studies of clomazone mode of action, *Pestic. Biochem. Physiol.*, 2006, **85**, 7–14, DOI: [10.1016/j.pestbp.2005.10.002](#).
 - 35 C. Mueller, J. Schwender, J. Zeidler and H. K. Lichtenthaler, Properties and inhibition of the first two enzymes of the non-mevalonate pathway of isoprenoid biosynthesis, *Biochem. Soc. Trans.*, 2000, **28**, 792–793, DOI: [10.1042/bst0280792](#).
 - 36 M. J. Konz, Herbicidal Isoxazolidine-3,5-diones, *US Pat.*, US4302238, 1981.
 - 37 X. W. A. Chan, C. Wrenger, K. Stahl, B. Bergmann, M. Winterberg, I. B. Müller and K. J. Saliba, Chemical and genetic validation of thiamine utilization as an antimalarial drug target, *Nat. Commun.*, 2013, **4**, 2060, DOI: [10.1038/ncomms3060](#).
 - 38 A. H. Y. Chan, I. Fathoni, T. Ho, K. J. Saliba and F. J. Leeper, Thiamine analogues as inhibitors of pyruvate dehydrogenase and discovery of a thiamine analogue with non-thiamine related antiplasmodial activity, *RSC Med. Chem.*, 2022, **13**, 817–821, DOI: [10.1039/D2MD00085G](#).
 - 39 A. H. Y. Chan, T. C. S. Ho, I. Fathoni, R. Pope, K. J. Saliba and F. J. Leeper, Inhibition of Thiamine Diphosphate-Dependent Enzymes by Triazole-Based Thiamine Analogues, *ACS Med. Chem. Lett.*, 2023, **14**, 621–628, DOI: [10.1021/acsmchemlett.3c00047](#).
 - 40 H. Jomaa, J. Wiesner, S. Sanderbrand, B. Altincicek, C. Weidemeyer, M. Hintz, I. Türbachova, M. Eberl, J. Zeidler, H. K. Lichtenthaler, D. Soldati and E. Beck, Inhibitors of the nonmevalonate pathway of isoprenoid biosynthesis as antimalarial drugs, *Science*, 1999, **285**, 1573–1576, DOI: [10.1126/science.285.5433.1573](#).
 - 41 K. Gupta and G. S. Saggi, *Isoprenoid Biosynthesis Pathway Enzymes as Promising Drug Candidates Against Malaria Parasites: An In-Silico Investigation*, Preprints.org, DOI: [10.20944/preprints202312.0032.v1](#), This is a preprint and has not been peer-reviewed.
 - 42 R. A. W. Frank, F. J. Leeper and B. F. Luisi, Structure, mechanism and catalytic duality of thiamine-dependent enzymes, *Cell. Mol. Life Sci.*, 2007, **64**, 892–905, DOI: [10.1007/s00018-007-6423-5](#).
 - 43 A. H. Y. Chan, T. C. S. Ho, K. Agyei-Owusu and F. J. Leeper, Synthesis of pyrrothiamine, a novel thiamine analogue, and evaluation of derivatives as potent and selective inhibitors of pyruvate dehydrogenase, *Org. Biomol. Chem.*, 2022, **20**, 8855–8858, DOI: [10.1039/D2OB01819E](#).
 - 44 A. H. Y. Chan, T. C. S. Ho, D. R. Parle and F. J. Leeper, Furan-based inhibitors of pyruvate dehydrogenase: SAR study, biochemical evaluation and computational analysis, *Org. Biomol. Chem.*, 2023, **21**, 1755–1763, DOI: [10.1039/D2OB02272A](#).
 - 45 A. H. Y. Chan, T. C. S. Ho and F. J. Leeper, Open-chain thiamine analogues as potent inhibitors of thiamine pyrophosphate (TPP)-dependent enzymes, *Org. Biomol. Chem.*, 2023, **21**, 6531–6536, DOI: [10.1039/D3OB00884C](#).
 - 46 A. H. Y. Chan, T. C. S. Ho and F. J. Leeper, Thiamine analogues featuring amino-oxetanes as potent and selective inhibitors of pyruvate dehydrogenase, *Bioorg. Med. Chem. Lett.*, 2023, 129571, DOI: [10.1016/j.bmcl.2023.129571](#).
 - 47 A. L. Hopkins, G. M. Keserü, P. D. Leeson, D. C. Rees and C. H. Reynolds, The role of ligand efficiency metrics in drug discovery, *Nat. Rev. Drug Discovery*, 2014, **13**, 105–121, DOI: [10.1038/nrd4163](#).
 - 48 N. A. Meanwell, Improving Drug Candidates by Design: A Focus on Physicochemical Properties As a Means of Improving Compound Disposition and Safety, *Chem. Res. Toxicol.*, 2011, **24**, 1420–1456, DOI: [10.1021/tx200211v](#).
 - 49 O. H. Wieland, The mammalian pyruvate dehydrogenase complex: Structure and regulation, *Rev. Physiol., Biochem. Pharmacol.*, 1983, **96**, 123–170, DOI: [10.1007/BFb0031008](#).
 - 50 A. Avdeef, The rise of PAMPA, *Expert Opin. Drug Metab. Toxicol.*, 2005, **1**, 325–342, DOI: [10.1517/17425255.1.2.325](#).
 - 51 R. A. Copeland, *Evaluation of Enzyme Inhibitors in Drug Discovery: A Guide for Medicinal Chemists and Pharmacologists*, Wiley, 1st edn, 2013, DOI: [10.1002/9781118540398](#).

